Regional and Global Estimation of Terrestrial CO_2 Exchange from NIGEC Flux Data

Final Report
December 2000

A. Scott Denning
Colorado State University, Fort Collins, CO

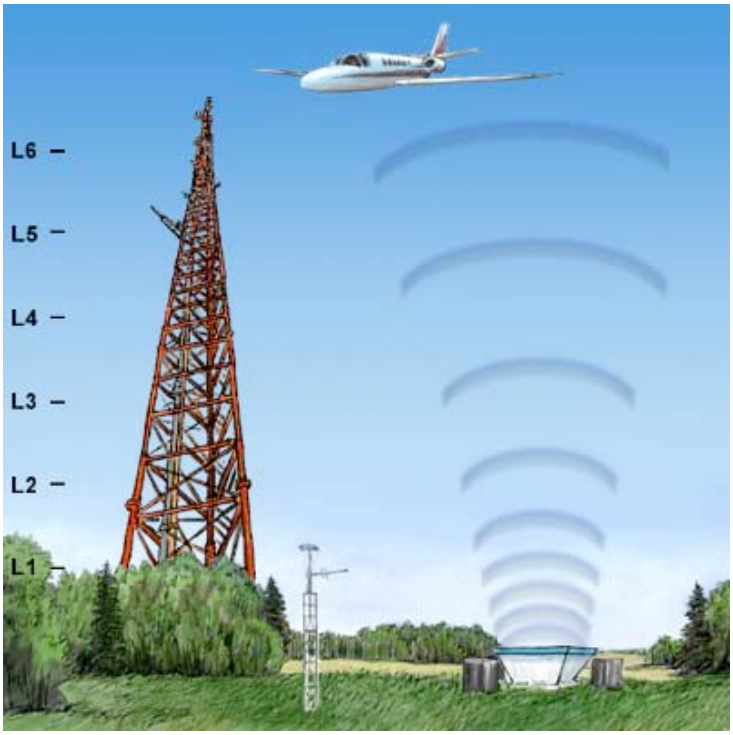

Executive Summary:

This investigation sought to bridge the gap between detailed eddy flux measurements made at local scales (for which regional representativeness is difficult to establish) and regional information provided by inversion studies (whose results are difficult to apply to particular ecosystems because of their coarse resolution). Inverting atmospheric observations using simulated tracer transport over vegetated land surfaces requires careful evaluation of interactions among surface energy budgets, ecosystem carbon flux, and atmospheric turbulence and convection (the "rectifier effect") which can confound the inversion procedure: we sought to evaluate this effect in nature and in a series of models. Technical and financial obstacles preclude a flux network of sufficient density to resolve sub-regional spatial patterns in carbon flux: we worked to develop a testable method for extrapolation of these fluxes using modeling, remote sensing, and atmospheric data.

We have coupled a self-consistent model (SiB2) of biophysical and biogeochemical exchanges at the land surface to local-scale turbulence models, to a mesoscale model, and to an atmospheric GCM. Vegetation is parameterized according to satellite imagery, and the models predict observable quantities such as energy fluxes and CO_2 concentrations. The coupled models are quite successful at predicting variations of latent and sensible heat fluxes, CO_2 fluxes, and CO_2 concentrations at multiple spatial scales. Simulations at the regional scale have been used to design sampling strategies for testing "bottom-up" estimates of fluxes using concentration measurements made from aircraft.

Objectives:

- Investigate the coupling between boundary-layer turbulence and forest ecophysiology, specifically the relationships among canopy conductance, photosynthesis, evapotranspiration, and sensible heat flux.
- Evaluate the realism and spatial scaling of the CO_2 "rectifier effect" in nature by using a hierarchy of simulations at increasing spatial scales to analyze simultaneous continuous measurements of surface carbon flux and the structure of the PBL over diurnal, synoptic, and seasonal time scales.
- Extrapolate the carbon flux measurements made at NIGEC-supported flux towers to the scale of single GCM grid cells (10^5 km^2) using remotely sensed vegetation data (LandSat TM and AVHRR NDVI) and gridded weather analyses to drive the improved biophysical model coupled to a mesoscale atmospheric model (RAMS).
- Use the improved land-surface model coupled to the global GCM, in conjunction with all the available observational data on atmospheric CO_2 concentration to estimate the global budget carbon budget of the atmosphere by inversion.

Approach:

Ecological and biogeochemical factors affecting the carbon balance of terrestrial ecosystems are heterogeneous in both space and time, complicating regional integration from site-based measurements. Spatial and temporal changes in atmospheric CO_2 contain information that can be used to extrapolate local ecological measurements to larger scales. Eddy flux towers provide estimates of ecosystem carbon balance over areas of several hectares. Extrapolation of carbon fluxes to larger scales is problematic because the terrestrial "signal" is convolved with atmospheric transport before it can be "received" by observers (e.g., aircraft or flask sampling networks) downwind. The signal-receptor relationship is further complicated by the fact that ecosystem carbon flux is not independent of atmospheric transport -- they interact through surface energy budgets, thermally-generated turbulence, and moist convection.

Denning et al. (1995) showed that inversions of the atmospheric CO_2 record using chemical tracer models have almost certainly underestimated global terrestrial carbon uptake because of inadequate representation of the coupling between ecosystem metabolism and turbulent mixing in the planetary boundary layer (PBL). Photosynthesis, PBL turbulence, and atmospheric convection over land are all forced by solar radiation at the surface, and they are therefore strongly correlated in nature, with strong ventilation and deeper mixing of CO_2-depleted air during the day and the growing season, and systematic retention of CO_2-enriched air under the nocturnal inversion and during the transition seasons. We found that the covariance between terrestrial photosynthesis, PBL structure, and cumulus convection produces a "rectifier effect," which results in a vertical gradient of several parts per million (ppm) in the annual mean CO_2 concentration over land (Denning et al., 1995, 1996b). This effect is strongest over the temperate and boreal latitudes of the northern hemisphere where vegetation and PBL turbulence are most strongly correlated on seasonal time scales and where the land area is greatest, and therefore produces a north-south gradient in annual mean CO_2 concentration at the locations of the observing stations (Conway et al., 1994). This purely natural meridional gradient is half as strong as that produced by the combustion of fossil fuels, and amounts to an "excess" of several ppm of CO_2 at high northern latitudes that is not observed. If the rectifier effect is realistic, a net sink of more than 3 GtC yr^{-1} is required in temperate and boreal ecosystems for consistency with the flask observations, which is nearly double the "consensus" estimate of the terrestrial sink (IPCC, 1995).

We conducted a hierarchical series of experiments to analyze the carbon balance of a "calibration" site that had been collecting data as part of the Ameriflux network: the WLEF TV transmitter tower in northern Wisconsin. The analyses evolved from being driven almost entirely by site data to a greater and greater reliance on remotely sensed data and gridded meteorological data, which are available everywhere. At each step of this process, we gained confidence in our ability to represent the mechanisms of carbon exchange and atmospheric transport in the modeling system.

We began with a detailed analysis of the carbon balance with SiB2, using local micrometeorological data to drive the calculation. These calculations were evaluated against the eddy correlation data available at the site, and used to derive site-specific parameters. The site-calibrated SiB2 model was then coupled to a mesoscale model (CSU RAMS) and used to perform a number of large-eddy resolving simulations (LES). These simulations were used to investigate the interactions between carbon fluxes, the surface energy budget, and PBL turbulence at the site. The predicted vertical structure was compared directly to the tower data for the lowest 400 m for the WLEF site. In addition, the LES runs were used to quantify the flux "footprint" of the tower, to investigate the contributions of the various vegetation types in the tower vicinity to the total flux. Next, we acquired a land-cover classification, a

LandSat Thematic Mapper image, and a series of AVHRR images of the vicinity of the site, and used these to parameterize SiB2 for the regional setting. In future NIGEC studies, we plan to use this information to continue performing simulations of the regional meteorology, carbon fluxes, and atmospheric CO_2 concentration using SiB2 coupled to RAMS, with a nested set of grids that allow direct comparison to local site data and consistency with analyzed regional weather. This will allow us to evaluate the effects of horizontal inhomogeneities on carbon fluxes, the surface energy balance, atmospheric transport and concentration of CO_2. The results of these simulations will allow quantitative evaluation of the rectifier effect and surface carbon balance at a spatial scale roughly corresponding to a GCM grid cell (10^5 km^2).

The improved model will make it possible to perform a global scale, multiyear simulation of atmospheric CO_2 transport and concentration driven by global NDVI data, and to use the results of that calculation to deduce the global carbon balance by inversion of the NOAA flask observations. Unlike previous calculations of this kind (e.g., Tans et al, 1990; Enting *et al* , 1995; Fan et al, 1998), such a calculation will be based on credible physical coupling between ecosystem metabolism and atmospheric transport, and will be consistent with the new data generated by NIGEC.

The WLEF-TV Tower Site

The Wisconsin forest site is the location of a 450 meter tall television transmission tower (WLEF-TV, 45° 55' N, 90° 10' W), located in the Chequamegon National Forest, 24 km west of Park Falls, WI. The region is in a heavily forested zone of low relief. The region immediately surrounding the tower is dominated by boreal lowland and wetland forests typical of the region. Much of the area was logged, mainly for pine, during 1860-1920, and has since regrown. The concentration of CO_2 has been measured continuously at 6 heights (11, 30, 76, 122, 244, and 396 m above the ground) since October, 1994, and CO_2 flux has been measured at three heights at this tower (30, 122 and 396 m) since 1996. Micrometeorology and soil temperature and moisture data are collected at the site or at the nearby USDA Forest Sciences Laboratory. During the summer of 1995, from March through October 1998 and throughout the growing season of 1999, a 915 MHz radar wind profiler has been operated at the site, which provided data on the height and structure of the PBL during the period. In conjunction with the vertically resolved CO_2 and flux data, the radar data provide a direct quantitative characterization of the CO_2 rectifier effect. Another significant advantage of this site is that the great height of the tower provides the opportunity for observing the carbon balance over a "footprint" that increases with height on the tower up to several km^2 for the highest observing platform, which is approximately two orders of magnitude greater than other Ameriflux monitoring sites. More information about the many data sets being collected at the site can be obtained from http://cheas.umn.edu.

Model Descriptions

The Simple Biosphere (SiB) Model, developed by Sellers et al. (1986), has undergone substantial modification (Sellers et al., 1996a, b), and is now referred to as SiB2. The number of biome-specific parameters has been reduced, and most are now derived directly from processed satellite data rather than prescribed from the literature. The vegetation canopy has been reduced to a single layer. Another major change is in the parameterization of stomatal and canopy conductance used in the calculation of the surface energy budget over land. This parameterization involves the direct calculation of the rate of carbon assimilation by photosynthesis, making possible the calculation of CO_2 exchange between the global atmosphere and the terrestrial biota on a timestep of several minutes (Denning et al, 1996a,b; Zhang et al, 1996). Photosynthetic carbon assimilation is linked to stomatal conductance and thence to the surface energy budget and atmospheric climate by the Ball-Berry equation (Ball, 1988; Collatz et al., 1991, 1992; Sellers et al., 1992, 1996a).

RAMS is a general purpose atmospheric simulation modeling system consisting of equations of motion, heat, moisture, and continuity in a terrain-following coordinate system (Pielke et al. 1992). The model has flexible vertical and horizontal resolution and a range of options that permit the selection of processes to be included (such as cloud physics, radiative transfer, subgrid diffusion, and convective parameterization). Two-way interactive grid nesting (Nicholls et al. 1995; Walko et al. 1995a) allows for a wide range of motion scales to be modeled simultaneously and interactively. For example, with nesting, RAMS can feasibly model mesoscale circulations in a large domain where low resolution is adequate, and at the same time resolve the eddy fluxes caused by juxtaposition of different land cover types, such as occur when irrigated cropland lies adjacent to drylands (Pielke et al. 1992).

Results:

Local-scale forest response to weather and climate

To test the biological model at the site, we required micrometeorological "forcing" data to be continuous (i.e., free of missing values of any variable for the period being simulated). Unbroken data sets are nearly impossible to produce due to instrument malfunctions, interruptions in electrical power, calibration problems, etc, so methods have been developed for "filling" the data. These include the use of ancillary data from nearby sites and statistical algorithms for interpolation in time and space. Using these methods and the data provided to us by the Davis and Bakwin NIGEC teams, we have produced unbroken time series of the variables listed in Table 1 for the period 1/1/1995 through 12/31/1998.

CO_2 concentrations (11, 20, 76, 122, 244, 396 m)
Wind speed (30, 122, 396 m)
Wind direction (30, 122, 396 m)
Air temperature (30, 122, 396 m)
Dew point temperature (30, 122, 396 m)
Vapor Pressure (30, 122, 396 m)
Air pressure
Incoming PAR
Precipitation
Total incoming radiation (short+long)
Net radiation
Incoming shortwave (VIS+NIR)
Incoming longwave

Table 1: Filled data for the WLEF tower. These data are available on our project web site at http://biocycle.atmos.colostate.edu/WLEF

The site meteorological data are used to "drive" the SiB2 model for actual conditions at the site. In this mode, the weather determines the fluxes of latent and sensible heat and CO_2 simulated by SiB2, but the fluxes do not feed back to influence the weather. This "SiBDRV" mode is useful for model development and testing, (because it runs very quickly), and for evaluation of new parameterizations.

Using these data, we have performed four-year simulations of the tower site with a 10-minute time step. Results of these simulations have been compared to observed soil moisture and temperature, snow depth and water content, and fluxes of heat, water, and CO_2. The results have been generally encouraging in terms of the diurnal and seasonal fluxes, though we have identified needed improvements for soil thermal and hydrological processes. Correct simulation of the rectifier effect for CO_2 requires that the covariance between the net ecosystem CO_2 flux and atmospheric transport be represented faithfully. Surface fluxes of CO_2 are well-represented in the model, including both seasonal and diurnal variations. The model tends to overestimate latent heat fluxes at mid-day relative to the observations in midsummer conditions. This could lead to underestimation of the energy available to drive turbulence. The Davis team has recently applied a correction for adsorbed water in the sampling tubes which has resulted in significantly increased latent heat flux in the revised data set (K. Davis, personal communication). This suggests the model may be performing better in this regard than shown in the figure.

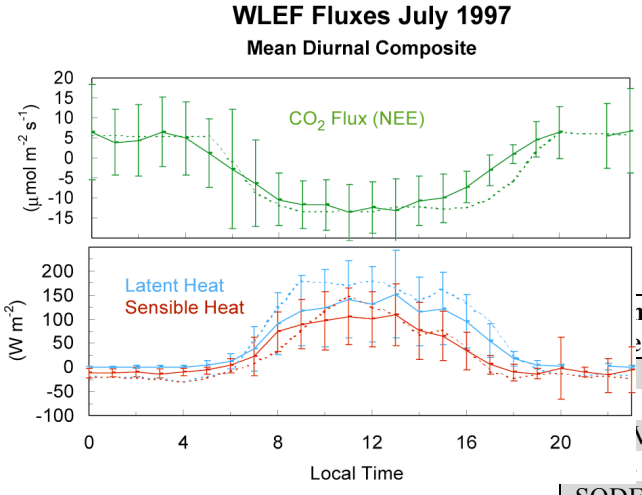

Figure 1: Diurnal cycles of fluxes of CO_2 (upper panel) and latent and sensible heat flux (lower panel). Solid lines show the observations, with 1σ "error bars" .
Dotted lines indicate model simulation.

neter	Parameter Description
	Canopy-top height
	Canopy-base height
VER	Vegetation cover
	Leaf angle distribution factor
SODEP	Soil depth
ROOTD	Rooting depth
PH	½ critical leaf water potential
TRAN11	Green-leaf transmittance (PAR)
TRAN21	Green-leaf transmittance (NIR)
TRAN12	Brown-leaf transmittance (PAR)
TRAN21	Brown-leaf transmittance (NIR)
REF11	Green-leaf reflectance (PAR)
REF21	Green-leaf reflectance (NIR)
REF12	Brown-leaf reflectance (PAR)
REF22	Brown-leaf reflectance (NIR)
VMAX	Rubisco velocity of sun-leaf
EFFCON	Quantum efficiency

The off-line "SiBDRV" model, forced with site meteorology, has also been used to investigate the sensitivity of the model to parameter values (Prihodko et al, 1998). This work (largely funded by a NASA graduate student fellowship to Ms. Lara Prihodko), included an investigation of the proper calibration of SiB2 for the WLEF site.

The "default" parameter values used to describe the vegetation at the site were derived from AVHRR vegetation imagery by Sellers et al (1996b) on a 1 x 1 degree global grid. We ran the model for June through August 1997 at the WLEF site 10,000 times with randomly perturbed parameter values and compared the simulated fluxes to the tower data to estimate "optimum" parameter values for the site. Surprisingly, the default parameter values derived from the satellite data produced one of the very best fits to the data out of the 10,000 realizations. The satellite-derived vegetation parameters are also generally consistent with those measured at the site by the Gutschick NIGEC team. This work is encouraging in terms of our overall objective of using satellite vegetation data to extrapolate carbon fluxes beyond the tower footprint at the regional scale.

Spatial Variation Of Vegetation And Soil Properties Controlling CO_2 Flux

We also generated gridded data sets of model parameters for SiB2 over a 1700 x 1700 km domain in the upper Midwestern USA from algorithms modified from Los *et al* (1994) using a vegetation classification derived by Hansen *et al* (2000), 10-day composite NDVI data from AVHRR imagery obtained from the EROS Data Center, and a soil texture database (STATSGO). The resulting dataset includes specification of mean values of 37 parameters (Table 2) for each month of the year on a regular 1 km grid centered at the WLEF-TV tower. We used this gridded dataset to specify vegetation and soils parameters for SiB and SiB-RAMS simulations.

Figure 2 shows an example of two parameter maps; the July leaf area index and the saturated soil moisture potential for the central part of the grid, which we have used for mesoscale simulation experiments (described below). We have derived all the parameters listed in Table 2 for each grid cell in the region at several different spatial resolutions (Fig 3), for use in a variety of coupled atmosphere-land surface experiments. These spatially-varying parameter sets allow for simulations of the immediate tower vicinity using eddy-resolving models for comparison to tower data. They further allow simulations of the regional environment and its interaction with heterogeneous land cover in mesoscale models, and global simulation in a GCM.

Table 2: SiB2 Model Parameters optimized for WLEF using Monte-Carlo analysis (Prihodko et al, 1998)

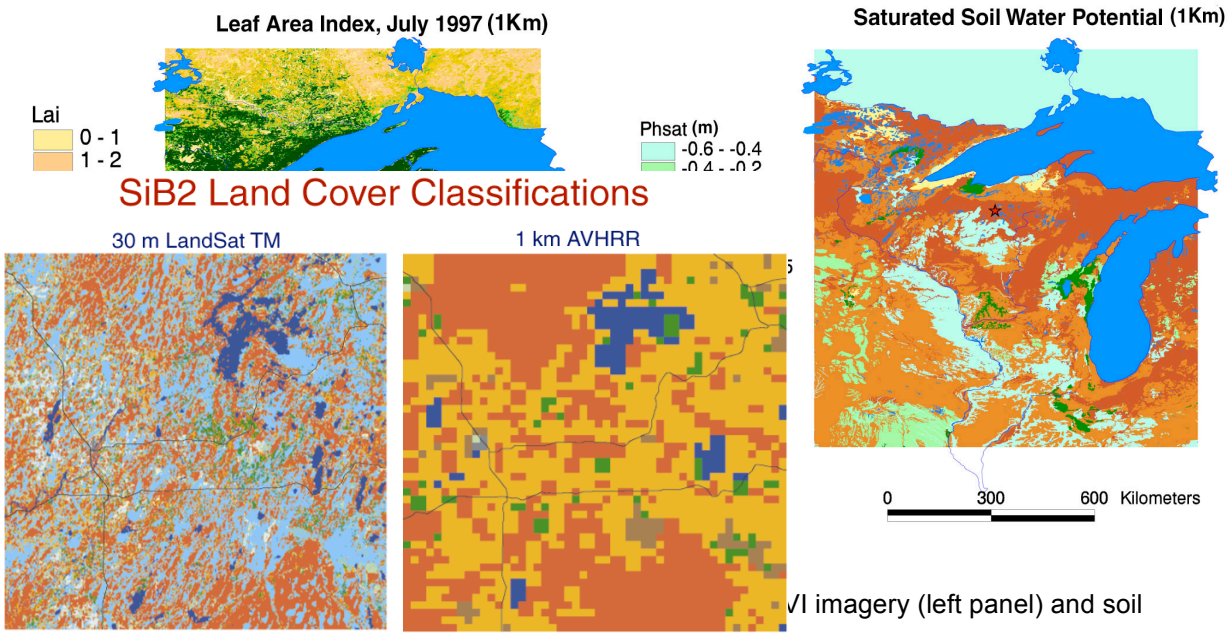

SiB2 Land Cover Classifications

VI imagery (left panel) and soil

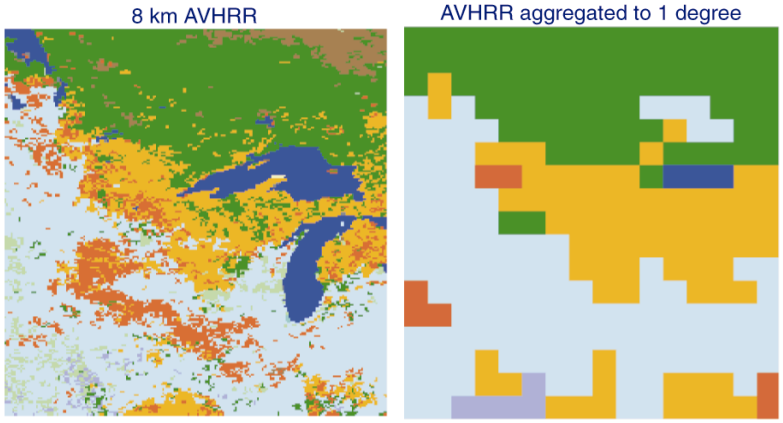

Figure 3: Vegetation classifications derived from satellite imagery centered at WLEF at 4 resolutions. Top panels are 50 km square; bottom panels are 1700 km square.

Forest-Atmosphere Interactions in the Tower Vicinity

We have coupled SiB2 to the mesoscale atmospheric model CSU-RAMS, and used the coupled model to investigate the interactions between the atmosphere and the underlying terrestrial ecosystems. The interactions simulated by the model include exchanges of energy, water, CO_2, and momentum, and are believed to impart observable "signatures" on the atmosphere over long distances. These interactions take place at many spatial scales, and we investigated the coupled system at regional and even global scales in 1999-2000. In 1998-99, we focused on the local tower vicinity because the tower data contains information on these interactions that we could use to test the performance of the coupled model.

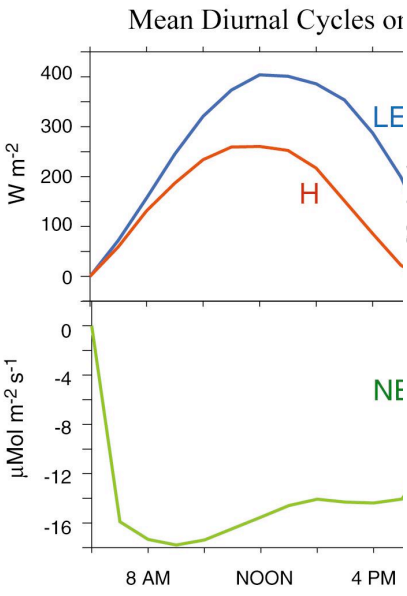

Figure 4: Simulated energy and carbo
km of the WLEF-TV tower.

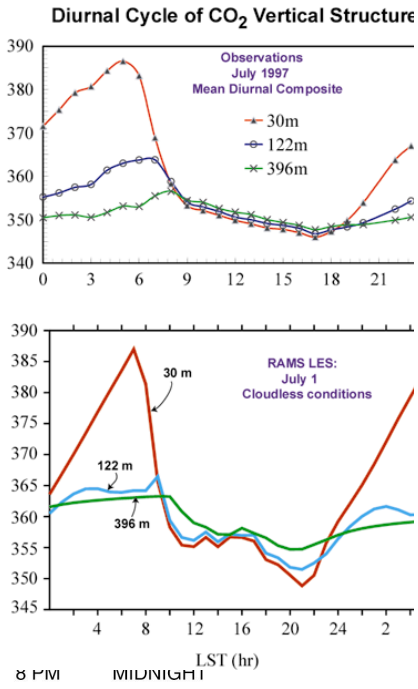

Figure 6: Timeseries of CO_2 concentration at 3 heights

A variable initialization nested grid simulation for the Wisconsin site was carried out using the coupled SiB-RAMS model for July 26, 1997. The model was configured with four grids with horizontal grid increments of 16 km, 4 km, 1 km, and 333 m. The widths of the four grids were 640 km, 150 km, 38 km, and 13 km. This configuration enables the representation of the larger scale synoptic features and by using successively finer grids telescopes down to the smaller scales in the region of the WLEF tower. The vertical grid increment was 60 m at the surface and was gradually stretched in the vertical to the top of the domain at 10 km. SiB parameters for nine vegetation classes were prepared at a 1 km resolution for the model domain and interpolated to model grid points. Surface elevation data was used to specify the topography for the four grids. NCEP reanalysis data and surface observations were used to prepare meteorological fields at six hourly intervals for the model domain. These fields were used to initialize the model at 6 a.m. local time and also to nudge the boundaries of the coarsest grid during the simulation. Surface winds were generally weak westerlies during the daytime and only a few clouds were present. For this particular simulation cloud microphysics was not activated, although we have begun testing the coupled SiB-RAMS model with clouds.

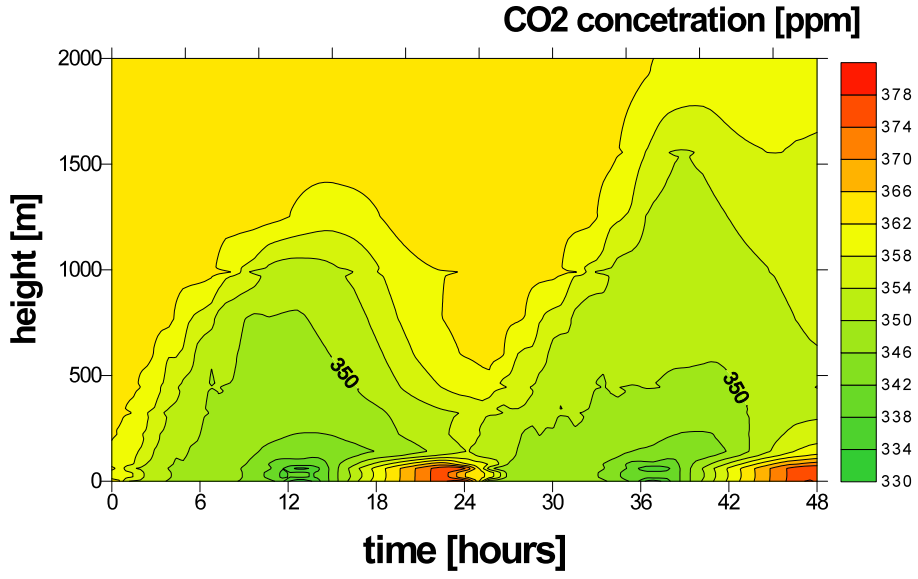

Figure 5: Vertical and temporal variations of simulated CO_2 concentration at the WLEF-TV tower location, as simulated on the finest grid nest.

Figure 4 shows the simulated diurnal cycles of the fluxes of sensible heat (H) , latent heat (LE), and CO_2 (NEE) averaged over more than 1500 grid cells in the innermost grid, which roughly corresponds to the flux footprint of the highest eddy covariance measurement level on the tower. These fluxes agree reasonably well with the mean diurnal cycles observed at the site, except that the simulated latent heat flux is much stronger than the data suggest. This may be the result of overly wet initialization of soil moisture, although the observed fluxes are known to be underestimated due to problems with instrumentation (Ken Davis, personal communication).

A time-height cross-section of the simulated CO_2 concentration in the vicinity of the WLEF-TV tower is shown in Figure 5, as simulated on the fine grid. Accumulation of high-CO_2 air under the nocturnal stable layer is followed in the morning by rapid mixing, and the daytime uptake of CO_2 by photosynthesis is felt through a much deeper convective boundary layer. The vertical variation in the amplitude and phase of the diurnal cycle is quite well captured relative to the observations (Fig 6), though the simulated vertical gradient is somewhat too strong during the day, and somewhat too weak at night.

Figure 7 displays the simulated energy fluxes at noon on the 1 km grid near the WLEF tower. The white areas are small lakes. Local variability of these fluxes of a factor of about two is caused by the heterogeneous vegetation cover. Fluxes of CO_2 also vary by about this much, and these variations in the surface energy budget lead to significant local forcing of turbulence and mesoscale circulations.

The simulated CO_2 concentration on the coarsest grid is shown at four times of day in Figure 8. Since there are no carbon fluxes from the water and winds are light, the initial concentration of 360 ppm over the Great Lakes are retained for some time (the orange/red areas in the 8 AM panel are Lakes Superior and Michigan). The strong carbon dioxide uptake by deciduous broadleaf forest leads to a minimum concentration south of Lake Superior by mid-day. This minimum deepens and spreads through much of the domain by evening, though concentrations remain high over the lakes. Respiration at night causes elevated concentrations in some areas, but over the central part of the domain the high-CO_2 air is too shallow to have much influence in this plot, which shows conditions 173 m above ground level. Interestingly, the daytime uptake of CO_2 by photosynthesis is not felt over the Great Lakes until late at night, when offshore drainage flow from the land replaces the initial 360 ppm air with lower concentrations. Vertical cross-sections of CO_2 concentration simulated on the coarsest (16 km) grid (Fig 9) show the diurnal evolution of the planetary boundary layer and its interaction with the variable land surface. The plots in this figure show concentrations averaged over the meridional direction. Growth of the convective boundary layer in the morning is accompanied by drawdown of the CO_2 by photosynthesis. The CBL reaches depths in excess of 1 km by midafternoon, with only weak vertical gradients of a few ppm from the surface up to this altitude. Near-surface concentrations reach a minimum in late afternoon, perhaps due to the collapse of sensible heat flux (turbulent decoupling) before the cessation of photosynthesis. At night, respiration produces very strong enhancement of CO_2 concentration in a shallow layer, with gradients in excess of 25 ppm at the top of this nocturnal stable layer, as have been observed at the tower. The CO_2-depleted air aloft is decoupled from this stable layer, and the residual low-CO_2 air is carried by advection and drainage flow toward the east over the Great Lakes. This half-cycle lag between terrestrial vegetation forcing and CO_2 response over the lakes is interesting, and may have implications for the atmospheric rectifier effect with respect to marine boundary layer measurements.

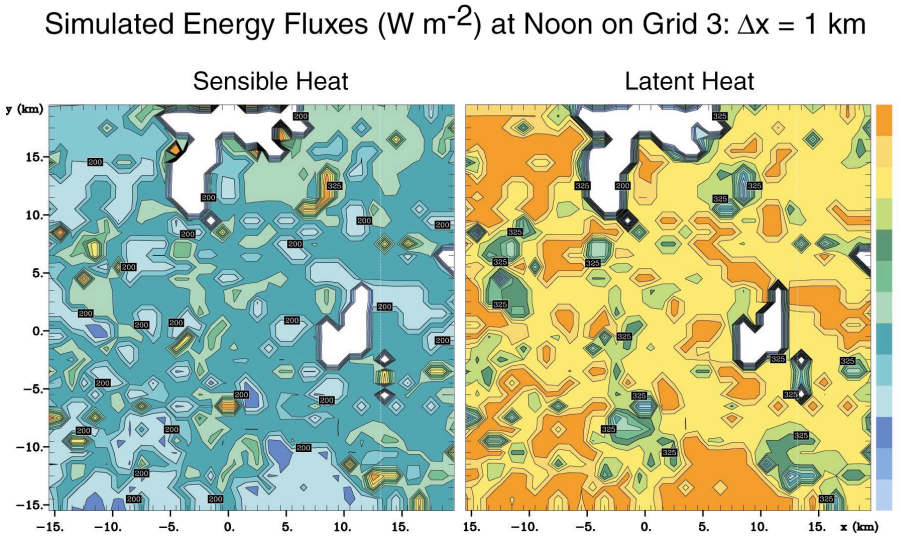

Figure 7: Spatial variations in simulated surface energy fluxes in grid 3, showing the effects of heterogeneous vegetation cover.

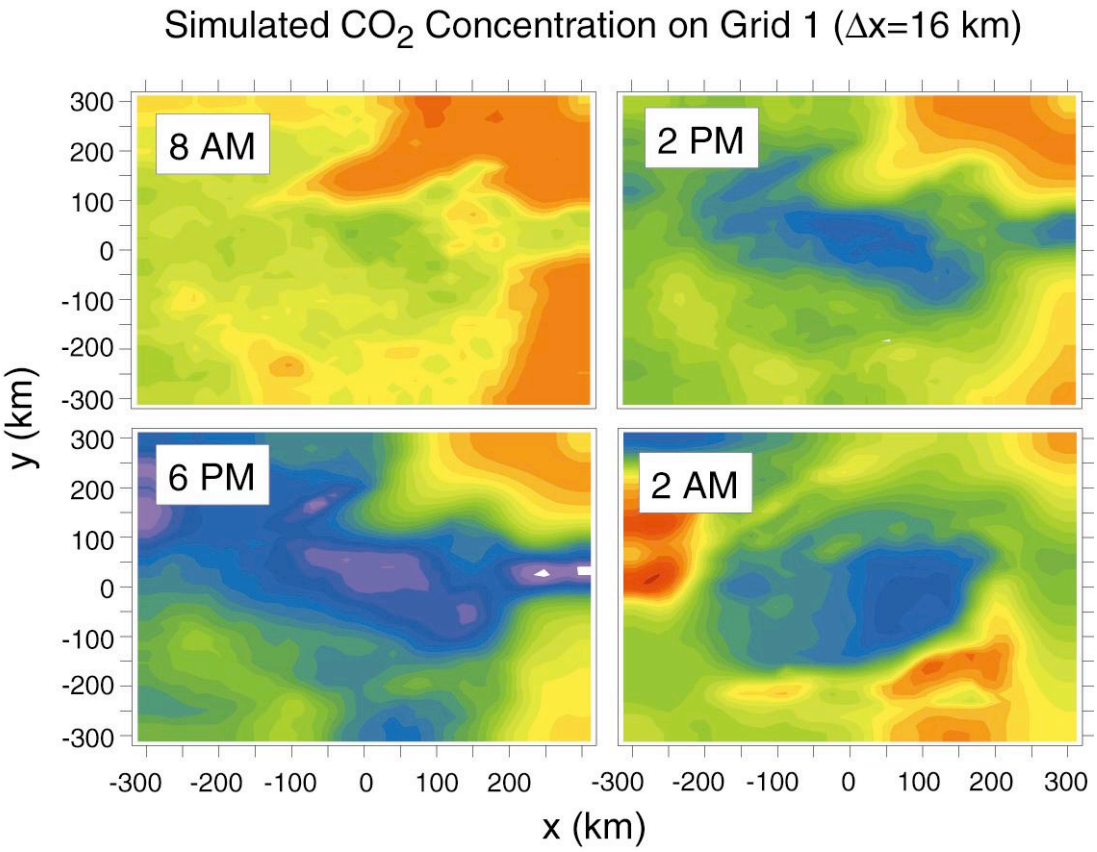

Figure 8: Simulated CO_2 concentration at 173 m AGL on the coarsest grid. Values range from 340 ppm (purple) to 365 ppm (red), with a contour interval of 1 ppm.

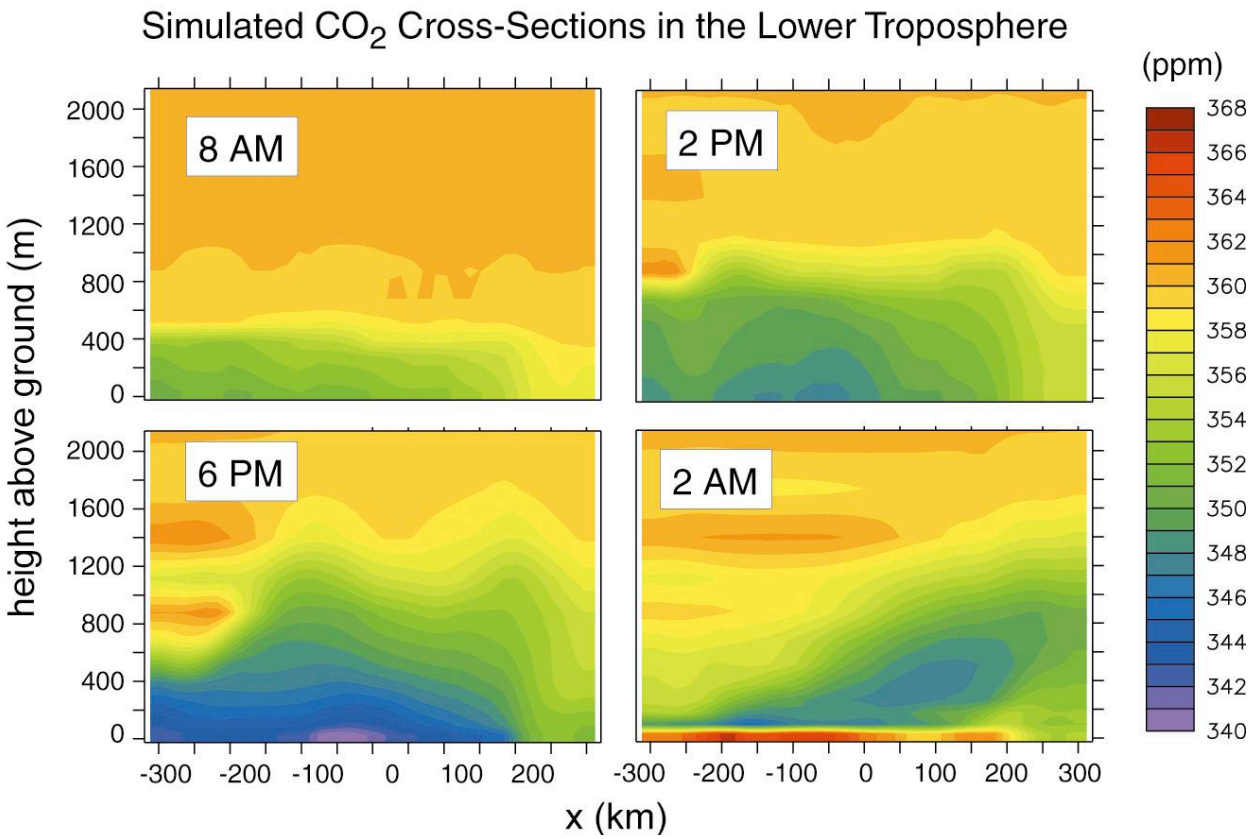

Figure 9: Diurnal evolution of simulated vertical structure of CO_2 on the coarsest grid

Lagrangian Particle Dispersion Modeling and Influence Function Analysis

One of the most basic questions about the forest-atmosphere interaction is what area of the underlying forest the flux measurements made at the tower represent. This area is known as the "flux footprint" of the measurements, and has been investigated by others using highly simplified representations of the atmospheric transport as a statistical mixing process. We have performed such an analysis using l
the advantage of a physically-based representation of the turb
horizontal homogeneity and stationary turbulence, and the ab
simulations have a horizontal grid spacing of 100 m, and a ve
released from the forest at each time step, and are "tagged" w
time, an upward "flux" of these particles is calculated at the l
is made of the fraction of the total flux that originated from e
time, the integral of the local flux from each grid cell is divid
conditional probability that the flux from each grid cell is me

An example of the results of such a calculation is shown in Fi
turbulence and a light background wind. Most of the flux mea
within 2 km of the tower, but the forest within 1 km of the to
upper level of the tower. This is because advection of air par
the nearby forest from reaching the eddy flux instruments bef
footprint at the top of the tower is enormous, stretching many
from almost completely disjoint portions of the underlying la
on the strength of the mean wind and the turbulence: they elo
decreasing turbulence. In 1999-2000, we worked closely wit
footprint analysis to investigate the fluxes of the various com

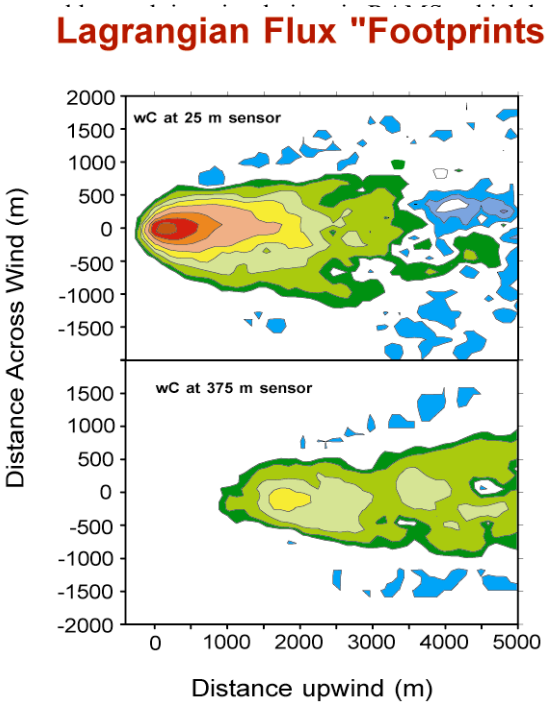

Figure 10: Footprints of eddy flux measured at two tower heights, as simulated by RAMS LES

Our footprint analysis system is under continuous development. Currently, it consists of the following components:

- **LPDM** (**L**agrangian **P**article **D**ispersion **M**odel) is the essential part of the system used to simulate atmospheric transport of passive tracer in scales ranging from the local scale (a few kilometers) to the continental one (thousands of kilometers) (Uliasz, 1994, Uliasz et al., 1996, Uliasz and Sorbjan, 1999). The tracer is represented by a large set of model particles that can be traced forward in time starting from sources or backward in time starting from receptors. The model allows us to represent atmospheric samples from various observing systems with different geometry and time averaging characteristics.
- **Interface to different meteorological models** and meteorological data. The LPDM is driven by an output from 3-dimensional meteorological models or analysis. The currently supported options include interfaces to:
  - multiple nested grid mesoscale or regional simulation with the CSU RAMS coupled with SiB2
  - RAMS configured for a single grid LES (Large Eddy Simulation)
  - climRAMS – a climatological version of RAMS for long term regional simulations,
  - CSU RAMS operational weather forecast
  - RUC (Rapid Update Cycle) gridded analysis fields from NCEP.
- **Footprint calculations** for observations of passive tracer concentrations and/or vertical fluxes**.** The footprints for concentration observations are derived from particle distributions. In addition, particle vertical velocities are used to flux footprints.
- **Sampling strategy evaluation** based on the Bayesian inversion technique (Uliasz, 2000).

Examples Of Concentration Footprints

The concentration footprints can be derived for different sampling period at the receptor. Figure **11** (top) shows a footprint calculated for tracer concentration observation at the 396 m level of the WLEF tower averaged over the entire month of August 1999. The surface fluxes were assumed constant in time. The LPDM can provide additional information about atmospheric transport, e.g., mean travel time between potential sources and a receptor (bottom). The model was driven in this simulation by the RUC gridded analysis fields. The RUC data have been archived every 1 hour at CSU for more than 1 year and are very useful for long term analysis. However, these fields do not represent very accurately vertical structure of the lower atmosphere and diurnal evolution of the atmospheric boundary layer. In particular, the footprints calculated for different tower levels show smaller differences than expected. The better results can be obtained from a nested grid RAMS with high resolution fine grid, especially, when RUC data are assimilated into the simulation.

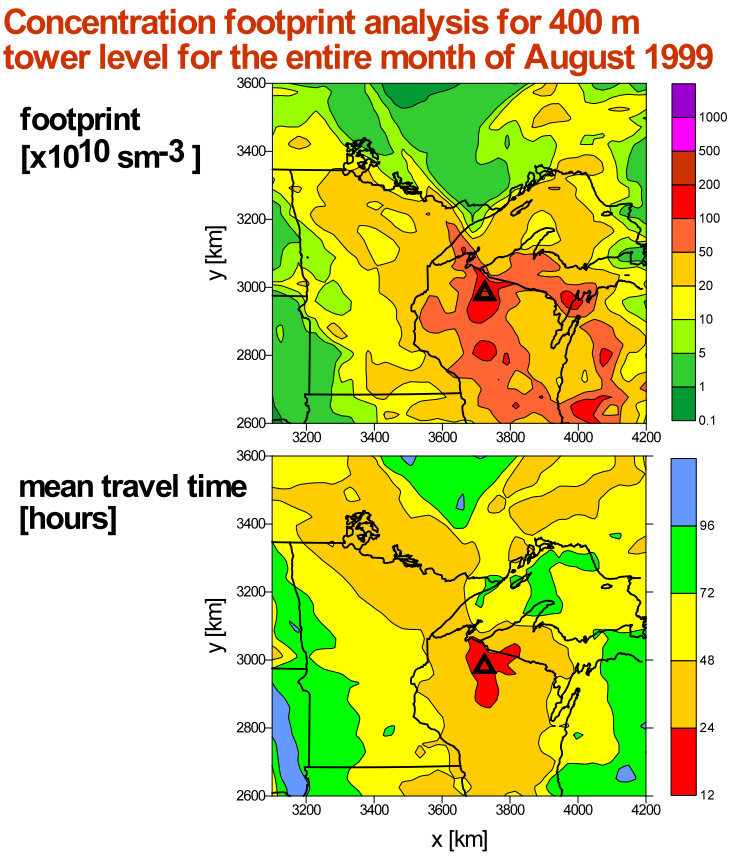

Figure 11: Influence functions calculations for WLEF.

Evaluation Of Sampling Strategies

The footprint approach can be used as a first step to interpret atmospheric data and to evaluate alternative sampling strategies. For a more formal comparison of sampling strategies we are using a Bayesian inversion technique (e.g., Tarantola, 1987). This method attempts to estimate unknown emissions from concentration data using some additional information: uncertainty of observational data and a-priori emission estimation and its uncertainty.

The cost function, *S*, is formulated in order to minimize distance between model results and observations and at the same time it does not allow the model to go too far from the a-priori emission estimation:

$$S(m) = (Gm - d_{obs})^T C_d^{-1} (Gm - d_{obs}) + (m - m_p)^T C_m^{-1} (m - m_p)$$

where m is the vector of emissions, m_p is a-priori emission estimation, G is the source-receptor matrix from the atmospheric model, d_{obs} is the vector of concentrations, C_d, C_m are covariance matrices representing uncertainty in observational data and initial emission estimation respectively, A^T, A^{-1} are transpose and inverse matrices. The new emission estimation is obtained as a correction to the initial one

$$\langle m \rangle = m_p + (G^T C_d^{-1} G + C_m^{-1}) G^T C_d^{-1} (d_{obs} - G m_p)$$

and, in addition, a new covariance matrix for emission can be calculated

$$C_m^* = (G^T C_d^{-1} G + C_m^{-1})^{-1}$$

We propose to use the reduction of uncertainty in emission estimation

$$\Delta C_m = C_m - C_m^*$$

as represented by the covariance matrices to compare different sampling strategies or different data sets from the point of view of information about surface emissions which can be retrieved from these data. It should be pointed out that concentration data are not necessary to calculate the uncertainty reduction ΔC_m. The required input for this algorithm includes:

- a sampling strategy – location and timing of atmospheric sampling,
- uncertainty of measurements,
- emission source configuration – their location and time characteristics, and
- uncertainty of initial emission estimation.

The source-receptor matrix must be provided by the atmospheric transport model.

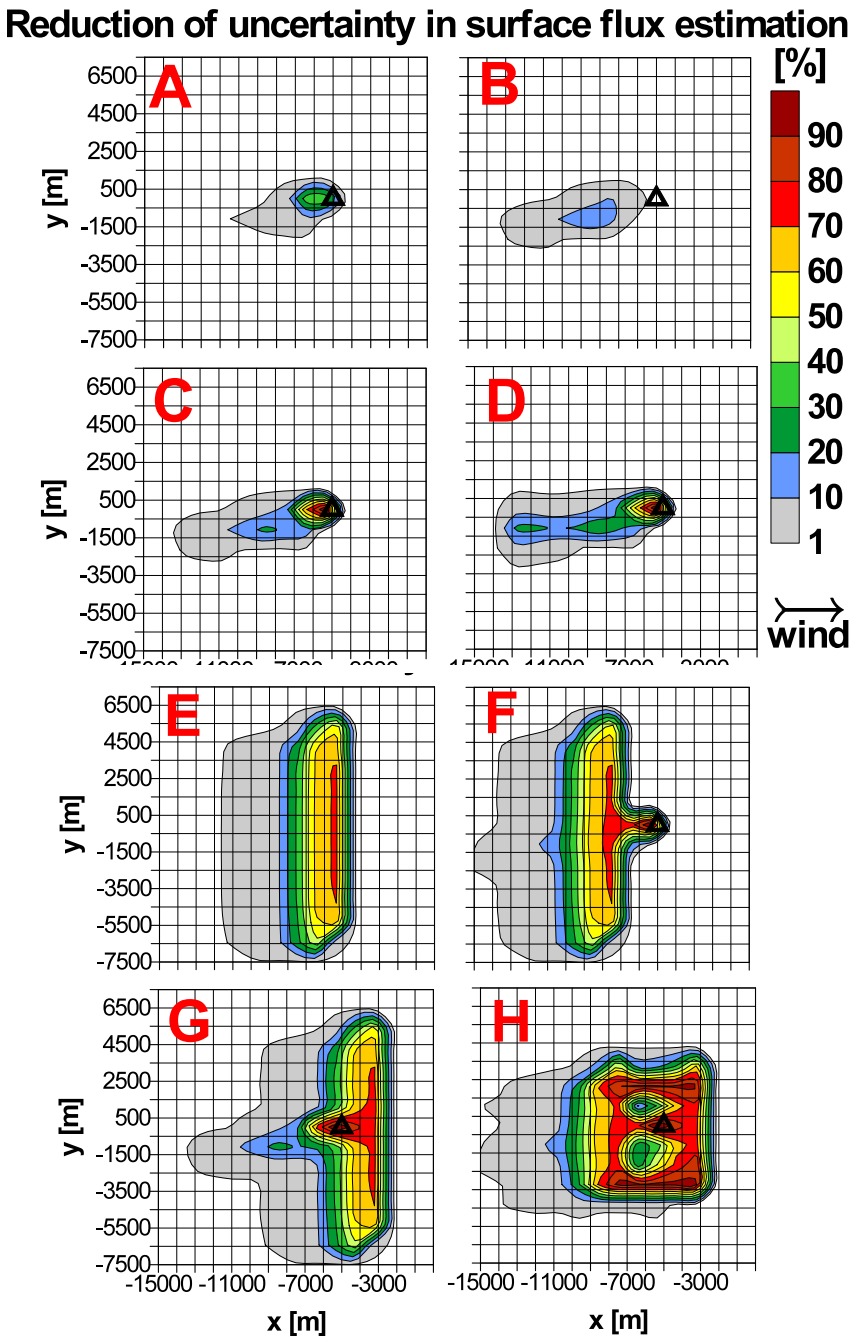

Figure 12: Reduction of uncertainty for Bayesian synthesis inversions of CO_2 flux performed on simulated pseudo-data using eight sampling strategies described in the text.

The method of evaluating sampling strategies is demonstrated on examples for moderately strong convective turbulence and a light background wind – a well developed late afternoon convective boundary layer over homogeneous terrain. The LPDM was coupled with RAMS model in the LES configuration to simulate transport of passive tracer released from the surface. This tracer can represent depletion of CO_2 concentration in the PBL due to local uptake by vegetation. For simplicity, the inflow fluxes of CO_2 were not considered in the analysis. Several sampling strategies were examined to find which provides the most information to estimate a grid of 1x1 km surface fluxes over 15x15 km domain. The results are presented as a reduction of uncertainty in surface emission estimation (Figure 12).

Sampling strategies:

A – a single sample at height z=100 m,

B – a single sample at height z=400 m. The uncertainty reduction is lower than in **B** but the footprint is larger.

C – 6 level tower: z =11, 30, 76, 122 244, 396m. This case corresponds to CO_2 concentration measurements at the WLEF tower. The uncertainty reduction is significantly higher in comparison to single samples **A** or **B**.

D - vertical profile through the entire boundary layer (e.g., tethered balloon): z = 50, 150, 250, …, 1650m. This sampling scenario provides more information and over a larger footprint than the tower samples in **C.**

E – 5 km long cross wind flight at z=100 m, samples every 200m The reduction of uncertainty is dramatically better than in the case of the single sample **A** taken at the same height. Only horizontal sampling can provide information on spatial distribution of CO_2 flux and its heterogeneity.

F – the same flight as in **E** but combined with the tower samples, the flight upwind of the tower. The tower is adding a significant amount of information.

G – the same flight as in **E** but combined with the tower samples, the flight downwind of the tower. This scenario seems to provide better uncertainty reduction than **F** and a somewhat more compact footprint.

H – the tower samples and the z=100 m flight around the tower along a rectangle (5 km cross wind, 4 km along wind). This is an example of a more complex flight pattern in the vicinity of the tower.

Further exercises indicated that an "envelope" flight pattern (in which samples are taken on a rectangle as in H above and diagonal flight legs are added) provides the most information for a given length of flight path. This approach can also be used to find an optimum height of aircraft samples. However, it was combined with another modeling study to answer the question whether CO_2 concentration variations due to landscape heterogeneity could be detected by a specific measurement system at a given height. In the above examples, the same accuracy was assumed for concentration data collected at the tower and by aircraft, however, it is possible to take into account differences in accuracy of various measurement systems. This approach also allows us to combine different types of measurement into analysis, e.g., measurements of CO_2 concentration and vertical flux or concentration measurements of different trace gases.

These analyses were provided to John Birks *et al* (University of Colorado NIGEC-funded researchers), who used them for flight planning for actual sampling flights with a light aircraft in August 2000.

Further tests were performed with the full inversion algorithm using a series of randomly generated emission fields and pseudo concentration data obtained as a perturbed model solution. The error (RMSE) of emission estimation in these tests corresponded quite well with the reduction of uncertainty in emission estimation in the above examples. It should be pointed out that the both uncertainty reduction and the error of emission estimation depend on uncertainty of the *a priori* emission and observational data. However, these measures can be still used for comparison of different sampling strategies even if the initial emission and data uncertainties are assumed in an arbitrary way. Application of the Bayesian inversion to estimate surface fluxes from observation will require a careful evaluation of data uncertainty, mismatch errors between model and observations and uncertainty of atmospheric transport model.

Products:

- Monthly georeferenced values on a 1 km grid of 37 SiB2 vegetation and soil parameters for a 1700 x 1700 km domain centered on the WLEF tower
- Hourly archive of weather and atmospheric transport data from NCEP Rapid Update Cycle (RUC) system since July 1, 1999
- Local and regional scale parameter sets for SiB2 at several resolutions
- Continuous micrometeorology record for WLEF-TV site [http://biocycle.atmos.colostate.edu/WLEF]
- Coupled SiB2-RAMS modeling system
- Lagrangian particle dispersion model driven from SiB2-RAMS simulations
- Footprint analysis system
- Site-calibrated SiB2 model for WLEF site

Papers/Presentations:

Denning, A. S., P.-L. Vidale, L. Prihodko, N. P. Hanan, K. J. Davis, and P. S. Bakwin, 1998. Simulations and Observations of Forest-Atmosphere Interactions Across Spatial Scales at the WLEF-TV Tower in Wisconsin, presented at Fall 1998 AGU Meeting, San Francisco.

Denning, A. S., N.P. Hanan, P.-L. Vidale, L. Prihodko, and N. Zhang, 1998. Regional Integration of Forest-Atmosphere CO2 Flux: a spatial hierarchy of atmospheric data and models. Presented at the Second FluxNet Conference, Polson, Montana, June, 1998.

Denning, A.S., Nicholls, M.E., P.-L. Vidale, M. Uliasz, N. Zhang, K.J. Davis, P.S. Bakwin, 1999. Simulations and Observations of Diurnal Coupling Between Ecophysiology and the Atmospheric Boundary Layer as a Control on CO_2 Concentrations. Presented at the Fall 1999 AGU Meeting, San Francisco.

Denning, A.S., Nicholls, M.E., P.-L. Vidale, M. Uliasz, N. Zhang, K.J. Davis, P.S. Bakwin, 1999. Atmospheric trace gas data in an integrated strategy to diagnose and understand the global carbon budget. Presented at the Spring 2000 AGU Meeting, Washington DC.

Potosnak, M. J., S. C. Wofsy, A. S. Denning, T. J. Conway, and D. H. Barnes, 1999. Influence of biotic exchange and combustion sources on atmospheric CO_2 concentrations in New England from observations at a forest flux tower. *Journal of Geophysical Research*, 104:9561-9569.

Prihodko, L., A. S. Denning, N. P. Hanan, G. J. Collatz, P. S. Bakwin, and K. Davis, 1998. Simulation and sensitivity analysis of carbon and energy fluxes at the WLEF-TV Tower site in Wisconsin, presented at Fall 1998 AGU Meeting, San Francisco.

Prihodko, L., A.S. Denning, M.E. Nicholls, P.-L. Vidale, T. Krebs, 1999. The Effects of Spatial Scale on Modeled Surface Fluxes. Presented at the Fall 1999 AGU Meeting, San Francisco.

Uliasz, M., 2000: Application of Lagrangian particle technique to modeling atmospheric transport in different scales: from LES to RAMS to GCM. *11th Joint Conference on the Applications of Air Pollution Meteorology with the A&WMA.* American Meteorological Society, 9-14 January, 2000, Long Beach, California.

Uliasz, M., A. S. Denning and N. Gimson, 2000: A modeling approach to design a mesoscale sampling campaign in order to estimate surface emissions. *11th Joint Conference on the Applications of Air Pollution Meteorology with the A&WMA.* American Meteorological Society, 9-14 January, 2000, Long Beach, California.

Uliasz, M., 2000: Influence Functions for Measurements of Tracer Concentration and Vertical Flux Derived from Lagrangian Particle Model. *Millenium NATO/CCMS International Technical Meeting on Air Pollution Modelling and Its Applications. 15-19 May 2000, Boulder, CO.*

Uliasz, M., 2000: A Modeling Approach to Evaluate Aircraft Sampling Strategies for Estimation of Terrestrial CO_2 Fluxes. *14th Symposium on Boundary Layers and Turbulence. American Meteorological Society, 7-11 August 2000, Aspen, CO.*

References:

Ball, J. T., 1988. An analysis of stomatal conductance. Ph.D. Thesis, Stanford University, Stanford, Calif.

Berry, J. A., Sellers, P. J., Randall, D. A., Collatz, G. J., Colello, G. D., Denning, A. S., Fu, W. and Grivet, C., 1998. SiB2, a model for simulation of biological processes within a climate model. In: Scaling Up (Eds. P. van Gardingen, G. Moody and P. Curran), Society for Experimental Biology, Cambridge University Press, in press.

Collatz, G. J., Ball, J. T., Grivet, C. and Berry, J. A., 1991. Physiological and environmental regulation of stomatal conductance, photosynthesis, and transpiration: a model that includes a laminar boundary layer. *Agric. and Forest Meteorol*., **54**, 107-136.

Collatz, G. J., Ribas-Carbo, M. and Berry, J. A., 1992. Coupled photosynthesis-stomatal conductance model for leaves of C4 plants. *Aust. J. Plant Physiol.*, **19**, 519-538.

Conway, T. J., P. P. Tans, L. S. Waterman, K. Thoning, D. R. Kitzis, K. A. Masarie, and N. Zhang, 1994: Evidence for interannual variability of the carbon cycle from the NOAA/CMDL global air sampling network. *Jour. Geophys. Res*., **99**, 22831-22855.

Denning, A. S., I. Y. Fung, and D. A. Randall, 1995: Latitudinal gradient of atmospheric CO_2 due to seasonal exchange with land biota. *Nature*, **376**, 240-243.

Denning, A. S., J. G. Collatz, C. Zhang, D. A. Randall, J. A. Berry, P. J. Sellers, G. D. Colello, and D. A. Dazlich, 1996a. Simulations of terrestrial carbon metabolism and atmospheric CO_2 in a general circulation model. Part 1: Surface carbon fluxes. *Tellus*, **48B**, 521-542.

Denning, A. S., D. A. Randall, G. J. Collatz, and P. J. Sellers, 1996b. Simulations of terrestrial carbon metabolism and atmospheric CO_2 in a general circulation model. Part 2: Spatial and temporal variations of atmospheric CO_2. *Tellus*, **48B**, 543-567.

Enting, I. G., Trudinger, C. M. and Francey, R. J., 1995. A synthesis inversion of the concentration and delta ^{13}C of atmospheric CO_2. *Tellus*, **47B**, 35-52.

Fan, S.-M., Gloor, M., Mahlman, J., Pacala, S., Sarmiento, J., Takahashi, T. and Tans, P.,1998. A large terrestrial carbon sink in North America implied by atmospheric and oceanic carbon dioxide data and models. *Science* **282**, 442-446.

Farquhar, G. D., von Caemmerer, S. and Berry, J. A., 1980. A biochemical model of photosynthetic CO_2 assimilation in C3 plants. *Planta*, **149**, 78-90.

Hansen, M., DeFries, R., Townshend, J. R. G. and Sohlberg, R., 1999, Global land cover classification at 1 km resolution using a decision tree classifier, *International Journal of Remote Sensing*, in press.

Intergovernmental Panel on Climate Change (IPCC), 1995. *Climate Change 1994: Radiative Forcing of Climate Change and an Evaluation of the IPCC IS92 Emission Scenarios* (eds. J. T. Houghton, L. G. Meira Filho, J. Bruce, H. Lee, B. A. Callander, E. Haites, N. Harris and K. Maskell). Cambridge University Press, Cambridge.

Los, S.O., C.O. Justice, and C.J. Tucker, A global 1 by 1 degree NDVI data set for climate studies derived from the GIMMS continental NDVI, *Int. J. Remote Sens*., **15**, 3493-3518, 1994.

Nicholls, M.E., R.A. Pielke, J.L. Eastman, C.A. Finley, W.A. Lyons, C.J. Tremback, R.L. Walko, and W.R. Cotton, 1995: Applications of the RAMS numerical model to dispersion over urban areas. *Wind Climate in Cities*, J.E. Cermak et al. Eds., 703-732.

Pielke, R. A., W. R. Cotton, R. L. Walko, C. J. Tremback, W. A. Lyons, L. D. Grasso, M. E. Nicholls, M. D. Moran, D. A. Wesley, T. J. Lee, and J. H. Copeland, 1992. A comprehensive meteorological modeling system RAMS.

Meteor. Atmos. Phys., **49**, 69-91.

Prihodko, L., A. S. Denning, N. P. Hanan, G. J. Collatz, P. S. Bakwin, and K. Davis, 1998. Simulation and sensitivity analysis of carbon and energy fluxes at the WLEF-TV Tower site in Wisconsin, presented at Fall 1998 AGU Meeting, San Francisco.

Sellers, P. J., Y. Mintz, Y. C. Sud, and A. Dalcher, 1986: A simple biosphere model (SiB) for use within general circulation models. *J. Atmos. Sci.*, **43**, 505-531.

Sellers, P. J., Heiser, M. D., and Hall, F. G., 1992. Relations between surface conductance and spectral vegetation indices at intermediate (100 m^2 to 15 km^2) length scales. *J. Geophys. Res*., **97**, 19033-19059.

Sellers, P. J., D. A. Randall, G. J. Collatz, J. Berry, C. Field, D. A. Dazlich, C. Zhang, and L. Bounoua, 1996a: A Revised Land-Surface Parameterization (SiB2) for Atmospheric GCMs. Part 1: Model formulation. *J. Clim*., **9**, 676-705.

Sellers, P. J., S. O. Los, C. J. Tucker, C. O. Justice, D. A. Dazlich, G. J. Collatz, and D. A. Randall, 1996b: A Revised Land-Surface Parameterization (SiB2) for Atmospheric GCMs. Part 2: The generation of global fields of terrestrial biophysical parameters from satellite data. *J. Clim*., **9**, 706-737.

Sellers, P. J., L. Bounoua, G. J. Collatz, D. A. Randall, D. A. Dazlich, S. O. Los, J. A. Berry, I. Fung, C. J. Tucker, C. B. Field, and T. G. Jensen, 1996c. Comparison of radiative and physiological effects of doubled atmospheric CO_2 on climate. *Science*, **271**, 1402-1406.

Tans, P. P., Fung, I. Y. and Takahashi, T., 1990. Observational constraints on the global atmospheric CO_2 budget. *Science* **247**, 1431-1438.

Tarantola, A.1987: Inverse Problem Theory – *Method for Data Fitting and Model Parameter Estimation*. Elsevier.

Uliasz, M., 1994: Lagrangian particle modeling in mesoscale applications. *Environmental Modelling II*, ed. P. Zannetti, Computational Mechanics Publications, 71-102.

Uliasz, M., 2000: A Modeling Approach to Evaluate Aircraft Sampling Strategies for Estimation of Terrestrial CO_2 Fluxes*. 14th Symposium on Boundary Layers and Turbulence. American Meteorological Society, 7-11 August 2000, Aspen, CO.*

Uliasz, M, R.A. Stocker,and R.A. Pielke, 1996: Regional modeling of air pollution transport in the southwestern United States. *Environmental modelling III*, ed. P. Zannetti, Computational Mechanics Publications, 145-182

Uliasz, M. and Z. Sorbjan,1999: Lagrangian statistics in the atmospheric boundary layer derived from LES. *13th Symposium on Boundary Layers and Turbulence.* American Meteorological Society, 10-15 January, 1999, Dallas, Texas. 281-282.

Walko, R.L., C.J. Tremback, R.A. Pielke, and W.R. Cotton,1995a: An interactive nesting algorithm for stretched grids and variable nesting ratios. *J. Appl. Meteor*., **34**, 994-999.

Walko, R. L, W. R. Cotton, J. L. Harrington, M. P. Meyers, 1995b: New RAMS cloud microphysics parameterization. Part I: The single-moment scheme. *Atmos. Res*., **38**, 29-621.

Zhang, C., D. A. Dazlich, D. A. Randall, P. J. Sellers, and A. S. Denning, 1996: Calculations of the global land surface energy, water, and CO_2 fluxes with an off-line version of SiB2. *Jour. Geophys. Res*., **101**, 19061-19075.